Updates to the
NRC gauge block interferometer

J. E. Decker[1], K. Bustraan[2], S. de Bonth[2], J. R. Pekelsky
Dimensional Metrology Program
Institute for National Measurement Standards (INMS)
National Research Council Canada (NRC)
Ottawa, CANADA   K1A 0R6

1 Introduction

Gauge blocks are calibrated traceable to the definition of the metre by using wavelengths of light recommended in the "Practical realisation of the definition of the metre," which lists radiations that can be used to define the metre [1]. The NRC gauge block interferometer (GBIF) is the instrument with which gauge blocks are calibrated in accordance with the ISO 3650:1998(E) gauge block standard [2] for Canadian industry, and in support of other calibration instruments in the NRC Dimensional Metrology Laboratory. Gauge block calibration is one of the primary methods for dissemination of the definition of the metre. This instrument was custom-built in-house, including hardware and software, and continues to undergo extensive testing exercises to build confidence in its world-class performance [3]. The instrument was initially conceived in the 1950's [4] and has gone through numerous upgrades and tests over the years. The last major software upgrade was in 1982, and hardware in 1997.

The NRC GBIF is upgraded in gradual stages between routine calibration work, since taking the GBIF off-line for a prolonged period of time is disruptive. Some strategy ideas for this kind of upgrade style are described in [5], which cites the NRC gauge block interferometer instrument and it's recent upgrade as a practical example. The present paper provides more detail on the hardware and software changes effected in the current series of upgrades, and mentions ideas planned for the on-going upgrade work. The GBIF instrument and calibration techniques on which these upgrades are based, are previously described in [6].

---

[1]207 M-36 Montreal Road, NRC, Ottawa, CANADA, K1A 0R6, tel. 613 991 1633, fax. 613 952 1394, e-mail: jennifer.decker@nrc.ca

[2]Department of Precision Engineering, Eindhoven University of Technology, Eindhoven, The Netherlands, tel. +31 40 247 3313, fax. +31 40 246 5330

2   NRC Gauge Block Interferometer Upgrades for 2000

The schematic diagram of the optical instrument, and procedures for wringing, set-up and measurement of the gauge blocks are described in detail in NRC Document No. 40002 [6]. This paper describes the hardware and software changes to that system.[3] Briefly, the NRC GBIF is a Michelson interferometer modified to use collimated light (Twyman-Green configuration). It is a custom-built instrument, designed and assembled in-house at the NRC. The inspiration for many of the recent improvements came as a result of the measurement uncertainty evaluation for gauge block calibration with this measuring system [7, 8], and in preparation for the pending addition of an infrared laser at nominal wavelength of 1.15 μm. Gauge block calibration procedures are largely unchanged following the software and hardware upgrades described herein.

2.1   Software Upgrades

2.1.1   Gauge Block Length Evaluation by the Technique of Exact Fractions

The definition of the length of a gauge block is the *perpendicular distance between any particular point of the measuring face and the planar surface of an auxiliary plate of the same material and surface texture upon which the other measuring face has been wrung.* [2]. The length of a gauge block ℓ includes the effect of one-face wringing. The NRC gauge block interferometer applies the technique of exact fractions [9, 10]. The basis of the method can be described mathematically by the following general expression:

$$\ell = m_1 \frac{\lambda_1}{2} = m_2 \frac{\lambda_2}{2} = \ldots = m_i \frac{\lambda_i}{2}, \tag{1}$$

where m_i are interference orders with integer κ_i and fractional F_i parts,

$$m_i = \kappa_i + F_i. \tag{2}$$

Solution of equation (1) for the value of length ℓ follows from knowledge of the wavelengths of light λ_i used to measure fractional interference orders F_i. The integer orders are determined using a regression-style software algorithm. The algorithm steps through test-length values, probing the match between the fractions evaluated from the test length, and the fractions that were measured, looking for the best match. One of the pitfalls of this technique is that there are several solutions for gauge block length ℓ, equation (1), to choose from. The criteria influencing the selection of the best solution, the one that represents the length of the gauge block, are: the number of wavelengths used and their nominal lengths, the calibration accuracy of the vacuum wavelengths, and the accuracy to which the fringe fractions are measured [11]. An expedient method for choosing the most likely solution for the gauge block length is to observe the fitting result graphically. A good quality measurement results in a characteristic symmetrical shape for the plot of fit parameter vs. length, with one solution displaying a distinct minimum compared to the others. This graphical representation allows quick operator judgement as to whether or not the fringe fraction readings F_i were acceptable, or should be repeated while the gauge block is still set up.

Because of the age of the programming language (Microsoft QuickBasic ca. 1980s), and the number of changes to hardware periferals, it was deemed more expedient to upgrade to a newer programming language dedicated to modular programming style, instrument control and data acquisition, rather than copy the original software onto the new platform. LabView software Version 5.0 was selected for this application because it is already being used with some experience in the Dimensional Metrology Laboratory, and it allows easy links

---

[3]NRC does not promote nor endorse any of the products or services named in this article.

with Microsoft Excel spreadsheets for effective display and storage of both raw data and evaluated values. In LabView vocabulary, computer programs are referred to as "virtual instruments" or simply VIs. The modular structure of the graphical programming language lends itself to effecting upgrades in well-defined steps, allowing verification of each measurement or evaluation task before continuing. This way, VIs representing instrument control and data analysis can be combined together to form the overall or 'root' instrument VI, representing the NRC gauge block interferometer instrument.

The new software uses a similar approach to the length evaluation algorithm as the old version. The software was written in stages. The first stage was the evaluation of length using vacuum wavelengths. The second stage included evaluation of refractive index of air (see below). Other modular VIs included: obliquity correction, thermal expansion correction, measurement of environmental temperature, air pressure and relative humidity, storing raw data, tables and graphs in Microsoft Excel software. Each VI was tested separately over a period of weeks, over the range of gauge block lengths and operators, to ensure that the output of the new version of the software matched the output of the old version. Upon combining these tested VIs to the overall GBIF VI, it was tested alongside the old version to ensure the high integrity of output for various measurement conditions and operators, before transfer of control from the old system to the new one.

### 2.1.2 Correcting Vacuum Wavelength for Refractive Index of Air

Upgrading the software in a series of tasks allows for the examination and testing of updates to empirical equations or constants. In gauge block calibration by optical interferometry, evaluation of the correction for the effect of the refractive index of air on the vacuum wavelengths of the light is the largest and one of the most important corrections to the overall gauge block length measurement. In most laboratories, this correction is evaluated by a series of empirical equations employing measured parameters of air temperature, air pressure, relative humidity and wavelength of light in vacuum. There are currently several versions of such equations in the literature, three of which are mentioned here. The differences between the Edlén equation updates of Birch and Downs [13], the equations by Bönsch [14] and Ciddor [15] have been compared, and acceptable agreement is found between the three methods, as shown in Figure 1. Nevertheless, the evaluation of the refractive index of air used by the GBIF has now been changed from the Edlén equation of [13] to that of Ciddor [15]. The primary incentive for this update is that Ciddor's formulae are valid for the wavelength range 300–1690 nm, whereas most other models have been verified only in the visible [13] or up to 780 nm wavelength [14]. Ciddor's version is more compatible with the 1.15 μm-wavelength laser addition to the GBIF, and is well within the uncertainty of the other models.

The versions of Birch & Downs [13], Bönsch [14] and Ciddor [15] were programmed in separate VIs in order to compare them with eachother. Measurements of check gauge blocks with history, over a range of lengths and laboratory conditions were done applying Ciddor's model. These results were compared with the evaluation of the same raw measurement data with the Birch & Downs model, and also NRC's 'old' software, to verify that the Ciddor VI does not have errors in any of the stages of its implementation. The difference between application of either of the two models for refractive index of air was shown to be typically less than 1 nm over the range of nominal lengths of our calibration service.

Input quantities to the Ciddor equations are vacuum wavelength (λ, μm), temperature (t, °C $= T - 273.15$ K), pressure (p, Pa), relative humidity $R\%$ and CO_2 content (x_c, ppm). Most equations for the refractive index of air consider the partial pressure of water vapour (p_w, Pa) rather than relative humidity. Relative humidity is defined as $R \equiv (p_w/p_{svp}) \times 100$ and fractional humidity $h = R/100$. The partial pressure of water vapour is determined from humidity measurement by taking the following BIPM density equation [16, 17] for the saturation vapour pressure

$$p_{svp} = e^{AT^2 + BT + C + DT^{-1}} \tag{3}$$

where the constants $A = 1.2378847 \times 10^{-5}$ [K^{-2}], $B = -1.9121316 \times 10^{-2}$ [K^{-1}], $C = 33.93711047$, $D = -6.3431645 \times 10^3$ [K].
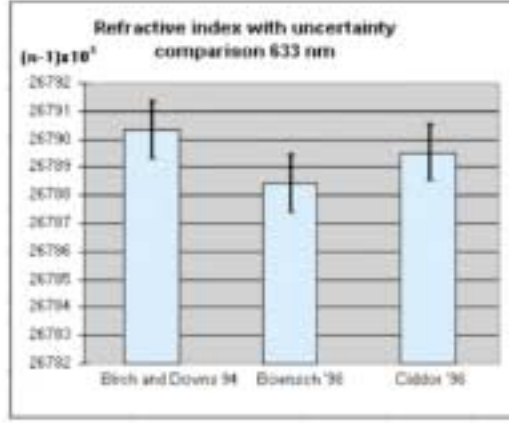
Figure 1: This plot compares the values of the refractive index of air, and their standard uncertainties, for three empirical equations. Each equation is evaluated for the same environmental conditions and 633 nm nominal wavelength. The models compared are: Birch and Downs [13], Bönsch [14] and Ciddor [15].

The refractive index of air is described by [15]

$$n_{prop} - 1 = \left(\frac{\rho_a}{\rho_{axs}}\right)(n_{axs} - 1) + \left(\frac{\rho_w}{\rho_{ws}}\right)(n_{ws} - 1). \tag{4}$$

Equation (4) represents a sum of the refractive index of dry air n_{axs} and the refractive index of pure water vapour n_{ws}, each weighted by a multiplicative factor that represents the ratio of the density of dry air ρ_a with respect to that of standard air ρ_{axs}, and the density of ambient moist air ρ_w with respect to the reference density of standard water vapour ρ_{ws}. Each of these terms is evaluated separately and substituted into equation (4) to yield the refractive index of the laboratory air; they are briefly described below.

The following two dispersion equations describe: the refractivity of pure water vapour

$$(n_{ws} - 1) \times 10^8 = 1.022(\,295.235 + 2.6422\,\sigma^2 - 0.032380\,\sigma^4 + 0.004028\,\sigma^6\,), \tag{5}$$

and the refractivity of standard air at 15 °C and 1 atm $= 101.325$ kPa

$$(n_{as} - 1) \times 10^8 = \frac{5792105}{238.0185 - \sigma^2} + \frac{167917}{57.362 - \sigma^2}, \tag{6}$$

where $\sigma = 1/\lambda$ is the wave number in $\mu\mathrm{m}^{-1}$ units. Now,

$$(n_{axs} - 1) = (n_{as} - 1)[1 + 0.534 \times 10^{-6}(x_c - 450)] \tag{7}$$

where x_c is the CO_2 content in parts per million.

The densities ρ_i are determined from the following general expression

$$\rho = \frac{p\,M_a}{Z\,R\,T}\left[1 - x_w\left(1 - \frac{M_w}{M_a}\right)\right], \tag{8}$$

where T is temperature in degrees Kelvin, x_w the molar fraction of water vapour (see below), M_a the molar mass of dry air in kg/mol, $M_w = 0.018015$ kg/mol is the molar mass of water, $R = 8.314510$ Jmol^{-1}K^{-1} the revised molar gas constant and Z the compressibility factor. The molar fraction of water vapour in moist air x_w is given by:

$$x_w = \frac{fhp_{svp}}{p}, \tag{9}$$

4

where $f = \alpha + \beta p + \gamma t^2$ is the enhancement factor of water vapour in air ($\alpha = 1.00062$, $\beta = 3.14 \times 10^{-8}$ Pa^{-1}, $\gamma = 5.6 \times 10^{-7}$ °C^{-2}). The molar mass of dry air M_a in [kg/mol] is given by:

$$M_a = [\, 28.9635 + 12.011 \times 10^{-6}(x_c - 400)\,] \times 10^{-3}. \tag{10}$$

The compressibility Z is given by the following general equation

$$Z = 1 - \left(\frac{p}{t}\right) [\, a_0 + a_1 t + a_2\, t^2 + (b_0 + b_1\, t)\, x_w + (c_0 + c_1\, t)\, x_w^2\,] + \left(\frac{p}{T}\right)^2 (d + e\, x_w^2) \tag{11}$$

where

a_0	$=$	1.58123×10^{-6}	KPa^{-1}	c_0	$=$	1.9898×10^{-4}	KPa^{-1}
a_1	$=$	-2.9331×10^{-8}	Pa^{-1}	c_1	$=$	-2.376×10^{-6}	Pa^{-1}
a_2	$=$	1.1043×10^{-10}	$K^{-1}Pa^{-1}$	d	$=$	1.83×10^{-11}	$K^2 Pa^{-2}$
b_0	$=$	5.707×10^{-6}	KPa^{-1}	e	$=$	-0.765×10^{-8}	$K^2 Pa^{-2}$.
b_1	$=$	-2.051×10^{-8}	Pa^{-1}				

Densities of standard air ρ_{axs} and standard water vapour ρ_{ws} are evaluated by making the appropriate substitutions in equation (8) and also using the compressibility of dry air Z_a (equation (11) where $T = 288.15$ K, $p = 101325$ Pa and $x_w = 0$) and the compressibility of standard water vapour Z_w (equation (11) where $T = 293.15$ K, $p = 1333$ Pa, and $x_w = 1$). Similarly, the density of the dry component of the laboratory air becomes

$$\rho_a = \frac{p\, M_a}{Z\, R\, T}\, (1 - x_w), \tag{12}$$

and the density of the water vapour component of the laboratory conditions is

$$\rho_w = \frac{p\, M_w}{Z\, R\, T}\, x_w. \tag{13}$$

Both of these latter two equations use the compressibility of the moist laboratory air determined by the laboratory conditions and equation (11).

The uncertainty evaluation of these equations is discussed in §4 below.

3   Hardware Upgrades

The control computer of the GBIF has been changed to a Pentium II computer (STD Model Platinum 166 Series). As mentioned above, the software is custom designed for the GBIF application. The computer communicates to the Hewlett-Packard Data Acquisition/Control Unit (Model 3497A) through a GPIB interface. Many of the peripheral sensor and control devices are connected to this scanner.

Several light sources provide the stable frequencies with traceability in accordance with the CIPM "*Mise en Pratique* of the Definition of the Metre (1992)" [1]. A commercially available polarization-stabilized single frequency He-Ne laser at 633 nm nominal wavelength (Coherent Tropel, Model 200) is calibrated at NRC against an iodine-stabilized He-Ne laser operating in accordance with the *Mise*. Two other He-Ne laser sources (TESA Division of Brown & Sharpe, Telford, UK) have nominal wavelengths of 612 nm and 543 nm. A He-Ne laser of 1.15 μm nominal wavelength, built in-house by the INMS Frequency and Time Program, is queued to be added on-line shortly. The light sources are being upgraded so as to replace the 114-cadmium lamp with laser sources which have better characteristics for image processing applications.

The beam-splitter has been replaced. The new beam-splitter is made of highest-grade fused silica for optical homogenaeity. It was polished and measured to $\lambda/100$ in flatness, and subsequently coated with a 50/50 beam-splitting coating by the Optical Components Group at the NRC. Custom optics to accommodate the

visible and near-infrared wavelengths of the GBIF collimators were also designed and fabricated in-house at NRC.

The optical fibre has been replaced with 0.16-Numerical Aperture silica multimode optical fibre of 200 μm core diameter (Thorlabs Model No. FG-200-UAT) terminated with SMA connectors. The change from 600 μm to 200 μm in fibre diameter results in a reduction of the obliquity correction by about an order of magnitude. Connectorizing the fibre improves the robustness of alignment and stability of the instrument for changing the fibre (a fibre of 400 μm diameter is also available for use on the instrument in the case that higher optical through-put is desired). The fibre end positioned with respect to the GBIF collimating lens serves as the point light source for the collimator optics (*i.e.*, on-axis and at the focus of the collimator). The mount holding the fibre end has been upgraded to improve the relative positioning of the fibre end with respect to the collimating optics. The other end of the optical fibre is mounted on the optical source table. All light sources are directed to this fibre end. Each light source is selected by activating individual shutters placed in the beam of each light source.

The GBIF uses bead-in-glass thermistors (VECO, SensiChip) calibrated by Thermometry at NRC for temperature measurement. The GBIF temperature measuring system is verified by probing a gallium fixed point cell. The gallium melting point is identified by the International Temperature Scale of 1990 (ITS-90) to define the SI temperature scale. The thermistor probes are placed in a gallium cell (cell made by the Thermometry Group at INMS) and the temperature is measured over the melting-point plateau, verifying that the temperature measurement of the GBIF system agrees with the 29.765°C fixed point of the cell. The absolute air temperature is measured with a combined standard uncertainty of 5 mK to a resolution of 1 mK (0.001°C). Typical air temperature drift is less than 10 mK per hour.

Temperature of long gauge blocks is determined by taking the average of measurements made by two thermistors. Each thermistor is fixed into a small copper block. The copper blocks are used as part of the support structure of the long gauge blocks, each positioned at one of the two Airy support points. A small amount of thermal paste between the gauge block side face and the copper block ensures good thermal contact. Temperature measurement of short gauge block calibrations applies one such thermistor-copper block contacted to a sample short gauge block in the neighborhood of the test arm of the GBIF.

Air pressure is measured using a Solartron Digital Pressure Module (Type DPM Model 7885–IM), calibrated by Mechanical Metrology at NRC. This is an improvement over the previous pressure gauge as the new gauge can be calibrated to an expanded uncertainty (k=2) of 10 Pa in absolute accuracy, compared to the previous 100 Pa. Furthermore, the secular stability of the new gauge is better than that of the capacitance monometer style of pressure gauge [12], providing increased confidence in its integrity between calibrations. Air pressure drift during gauge block measurements generally follows the ambient atmospheric conditions.

4   Measurement Uncertainty

The measurement uncertainty is evaluated following the rules of the *Guide to the Expression of Uncertainty in Measurement* [18] or GUM. The GUM groups statistical evaluation of uncertainty as Type A, and all other forms of uncertainty evaluation as Type B. In the terminology of the GUM, standard uncertainty is equal to, or is the analogue of one standard deviation. The combined standard uncertainty is the sum of squared standard uncertainty components. Each component represents the standard uncertainty attributed to each factor that influences the outcome of the measurement. The influence parameters and the standard uncertainties listed in Table 1 represent best measurement capability at NRC. Length dependent and end-effect uncertainties are summed separately in quadrature, and combined as a final step in the evaluation of the expanded uncertainty $U = ku_c$, where $k = 2$.

Standard uncertainties $u(x_i)$ listed in Table 1 are evaluated from characterization experiments performed in-house on the NRC gauge block interferometer, calibration certificates from sensor calibrations, or manufacturers specifications. The detail of this uncertainty evaluation is described in [8].

Influence Factor x_i	Physical Standard Uncertainty $u(x_i)$	Contribution to Length Uncertainty $c_{x_i}u(x_i)$ /nm
Fraction measurement (Type A)	0.01 fringe	2
Wringing (Type A)	6 nm	6
Phase-change	10 nm	10
Gauge block flatness and parallelism	2 nm	2
Interferometer optics:		
Wavefront errors	3 nm	3
Obliquity:		
source size	3.5 μm	$0.001L$
alignment higher-order	$(0.3/\sqrt{3})$ mm	$0.1L$
He-Ne laser:		
1-year drift	0.01 ppm	$0.005L$
calibration	0.002 ppm	$0.001L$
Thermal dilatation coefficient†	1 ppm/K	$0.005L$
Gauge temperature†:		
calibration	2 mK	$0.023L$
drift	4 mK	$0.046L$
gauge gradient	6 mK	$0.069L$
reading resolution	1 mK	$0.012L$
higher order term		$0.008L$
Refractive Index of Air:		
Ciddor equation	0.01 ppm	$0.010L$
Air pressure		
calibration	5 Pa	$0.014L$
reading capability	1 Pa	$0.003L$
drift	3 Pa	$0.008L$
Air temperature		
calibration	2 mK	$0.002L$
reading capability	1 mK	$0.001L$
drift	4 mK	$0.004L$
Humidity		
accuracy	1.2%	$0.010L$
reading capability	0.1%	$0.001L$
drift	1%	$0.009L$
Expanded Uncertainty (k=2):		$2\sqrt{12.4^2 + 0.144^2L^2}$ nm

ppm: parts per million $= 10^{-6}$

†Assumes steel gauge block, $\alpha = 11.5$ ppm/K and 50 mK temperature deviation from 20°C.

Table 1: Standard uncertainties attributed to best measurement capability of gauge blocks in the NRC gauge block interferometer, where L is in millimetres. A coverage factor of $k = 2$ is used for the expanded uncertainty. All uncertainty evaluations are Type B, except where noted in the table.

The standard uncertainty of the empirical equations for the refractive index of air is quoted by Ciddor to be 1×10^{-8} — the same as that quoted for the other models. With the change in the equation for the evaluation of refractive index, it is necessary to confirm that the sensitivity coefficients for the uncertainty evaluation represent the same functional dependence as for the previous equation for refractive index. The equations of Ciddor are many, and complex enough that the evaluation of the sensitivity coefficients in an analytical manner would be arduous. Therefore, n_{prop} of equation (4) was plotted for variations in each of the input parameters x_i to determine the slope m of the refractive index $n_{prop} = mx_i + b$. Evaluated refractive index was plotted for parameters of air temperature ($x_i = t$), pressure ($x_i = p$), relative humidity ($x_i = RH$) and vacuum wavelength ($x_i = \lambda$). All of the plots were linear within the range of experimental conditions that would typically be observed in the laboratory. As expected, the values of the sensitivity coefficients determined in this way are the same as the those determined in the analytical evaluation for the Edlén equation [8].

5   Summary

Recent hardware and software updates to the NRC gauge block interferometer are described. These, and ongoing upgrades to the instrument, result in improved confidence in the calibration of short and long gauge blocks. Upgrades to be brought on-line shortly include the application of phase-shifting and image processing techniques to the interference fringe analysis, custom designed optical elements and the addition of a new infrared laser source.

6   Acknowledgements

References

[1] Quinn, T.J., 1999, "Practical realisation of the definition of the metre (1997)," *Metrologia*, **36**, pp. 211–244.

[2] ISO 3650:1998(E), 1998, 2nd Edition 1998-12-15, (International Organization for Standardization (ISO) Central Secretariat, Switzerland, Internet iso@iso.ch).

[3] Decker, J.E., Lapointe, A., Stoup, J., Viliesid Alonso, M., Pekelsky, J.R., 1999, "NORAMET comparison of gauge block measurement by optical interferometry," *Metrologia*, **36**, pp. 421–432.

[4] Baird, K.M., 1957, "Calibration of gauge blocks in Canada," Proceedings of a Symposium on Gage Blocks, NBS August 1955, National Bureau of Standards Circular 581, pp. 21–25.

[5] Decker, J.E., Bustraan, K., de Bonth, S., Pekelsky, J.R., " Improving the quality of your measurement system by bringing it up to date," presented at the 2000 NCSL Workshop and Symposium, Toronto, CANADA, 16–20 July 2000.

[6] Decker, J.E. and Pekelsky, J.R., "Gauge Block Calibration by Optical Interferometry at the National Research Council Canada," presented at the Measurement Science Conference, Pasadena, CA, Janurary 1997. National Research Council of Canada (NRC), Ottawa, Canada Report No. 40002, 17 pages.

[7] Decker, J.E. and Pekelsky, J.R., 1996, "Uncertainty evaluation for the measurement of short gauge blocks by optical interferometry," National Research Council of Canada (NRC), Ottawa, Canada Report No. 41374, 26 pages.

[8] Decker, J.E. and Pekelsky, J.R., 1997, "Uncertainty evaluation for the measurement of short gauge blocks by optical interferometry," *Metrologia*, **34**, pp. 479–493.

[9] Born, M. and Wolf, E., 1980, Principles of Optics, 6th ed., (Pergamon Press, New York), pp. 286–306.

[10] Hariharan P., 1992, Basics of Interferometry, (Academic Press, Inc., New York), Chapter 8.

[11] Siemsen, K.J., *et al.,* 1996, "A multiple frequency heterodyne technique for the measurement of long gauges," *Metrologia*, **33**, pp. 555–563.

[12] Bowman, W.P. *private communication.*

[13] Birch, K.P. and Downs, M.J., 1994, "Correction to the updated Edlén equation for the refractive index of air", *Metrologia*, **31**, pp. 315–316.

[14] Bönsch, G. Potulski, E., 1998, "Measurement of the refractive index of air and comparison with modified Edlén's formulae", *Metrologia*, **35**, pp. 133–139.

[15] Ciddor, P.E. 1996, "The refractive index of air: new equations for the visible and near infrared", *Applied Optics*, **35**(9), pp. 1566–1573.

[16] Giacomo P., 1982, "Equation for the determination of the density of moist air (1981)," *Metrologia*, **18**, pp. 33–40.

[17] Davis R.S., 1992, "Equation for the determination of the density of moist air (1981/1991)," *Metrologia*, **29**, pp. 67–70.

[18] "Guide to the expression of uncertainty in measurement", 1993, 1st Edition (International Organization for Standardization, Switzerland), 101 pages.